Erschienen in: SiliconPV 2019, The 9th International Conference on Crystalline Silicon Photovoltaics : 8-10 April 2019, Leuven, Belgium / Poortmans, Jef et al. (Hrsg.). - Melville, New York : AIP Publishing, 2019. - (AIP Conference Proceedings ; 2147,1). - 040018. - ISBN 978-0-7354-1892-9
http://dx.doi.org/10.1063/1.5123845

Compensation of the Sputter Damage During a-Si Deposition for poly-Si/SiO_x Passivating Contacts by Ex-Situ P-Doping

Jonathan Steffens[a)], Johannes Rinder[b)], Giso Hahn[c)], Barbara Terheiden[d)]

University of Konstanz, Department of Physics, 78457 Konstanz, Germany

[a)]Corresponding author: jonathan.steffens@uni-konstanz.de
[b)]johannes.rinder@uni-konstanz.de
[c)]giso.hahn@uni-konstanz.de
[d)]barbara.terheiden@uni-konstanz.de

Abstract. The rf magnetron sputter deposition of a-Si during fabrication of passivating contacts based on poly-Si on top of an interfacial silicon oxide (poly-Si/SiO_x) and a possible sputter damage is investigated, as it is also observed during transparent conductive oxide sputtering for heterojunction solar cells. It is shown that the high temperature anneal for partial crystallization of the sputtered a-Si has a detrimental effect on passivation quality. However, doping during partial crystallization of the a-Si layer by a $POCl_3$-diffusion compensates this decrease of passivation quality by a field effect passivation. Moreover, a subsequent hydrogenation of the interface leads to implied open circuit voltages of up to 719 mV and saturation current densities of down to 9 fA/cm^2. Furthermore, depth profiles of the dopants measured by glow discharge optical emission spectroscopy (GD-OES) and electrochemical capacitance-voltage profiling (ECV) reveal a significant difference between total (~$3.5 \cdot 10^{21}$ cm^{-3}) and electrically active (~$5 \cdot 10^{20}$ cm^{-3}) phosphorous atomic density in the poly-Si layer. From these depth profiles also a pile-up of electrically inactive phosphorous close to, but a few nanometers off the interfacial oxide was observed.

INTRODUCTION

Recently, passivating contacts based on doped poly-Si layers on top of an interfacial oxide (poly-Si/SiO_x) have evolved into a concept for high efficiency solar cells [1]. Usually, amorphous silicon (a-Si) is deposited first and subsequently crystallized to poly-Si at temperatures above 800°C. Several a-Si deposition techniques are applied, e.g. chemical vapour deposition [2], electron beam evaporation [3] or sputter deposition [4]. Up to now it is not clear which technique will be the future standard to produce high efficiency solar cells and at the same time offer a sufficient industrial throughput. In this contribution, the a-Si deposition by rf magnetron sputtering is investigated as this technique is already established for high industrial throughput [5].

One challenging issue is a possible sputter damage to the passivated interface, as it also occurs during sputtering of transparent conductive oxides for heterojunction solar cells. There are two main sources of this damage, first plasma irradiation by high energy photons and second particle bombardment by sputtered atoms, electrons, ions and at the target neutralized and reflected Ar atoms [6]. The strength of these damage sources can be controlled by the sputter parameters, i.e. low plasma power, high plasma pressure, large target-sample distance and high substrate temperature [6,7].

In this study, the sputter damage to a poly-Si/SiO_x passivating contact during a-Si sputter deposition and its compensation is investigated. In this context, depth profiles of the total and electrically active dopant atomic density are discussed.

SiliconPV 2019, the 9th International Conference on Crystalline Silicon Photovoltaics
AIP Conf. Proc. 2147, 040018-1–040018-5; https://doi.org/10.1063/1.5123845
Published by AIP Publishing. 978-0-7354-1892-9/$30.00

EXPERIMENTAL

The used substrate was 250 µm thick n-type silicon floating zone material with a base resistivity of 200 Ωcm cut into 5x5 cm^2 pieces. Immediately after a short dip in hydrofluoric acid (HF), an interfacial oxide was thermally grown with a thickness of roughly 2.5 nm. a-Si layers with a thickness of approximately 75 nm were rf magnetron sputtered successively on both sides of the samples with a pure argon plasma applied to an undoped silicon target with a purity of 99.999%. In contrast to chemical vapour deposited a-Si layers, the sputtered layers can be considered as basically hydrogen-free, as there was no hydrogen gas added to the plasma. The sputter parameter set was optimized with respect to a trade-off between low sputter damage and a sufficient deposition rate.

One group of these samples was annealed in a quartz tube furnace in N_2 atmosphere to partially crystallize the intrinsic a-Si layers, while the other group was annealed in a $POCl_3$-diffusion to additionally dope the layers. Both high temperature anneals were operated above 900°C for 30 min immediately after an H_2O_2/HCl and HF cleaning process. Afterwards, the grown phosphorous silicate glass (PSG) was removed from the $POCl_3$-diffused group with HF. As this PSG grows into the layer, the HF etch reduces the doped poly-Si layer thickness to 67 nm, which was measured by spectral ellipsometry. For hydrogenation, on one half of the samples a hydrogen-rich silicon nitride (SiN_x) was plasma-enhanced chemical vapour deposited on both sides and a subsequent firing step was performed in a belt furnace at a peak set temperature of 910°C to release hydrogen from the silicon nitride layer to the poly-Si/SiO_x interface for defect passivation.

All samples were characterized by photoconductance decay (PCD) measurements in terms of implied open circuit voltages iV_{oc}, saturation current densities J_0 and sheet resistance R_s. In addition, depth profiles of the total phosphorous atomic density and uncalibrated oxygen content were simultaneously measured using glow discharge optical emission spectroscopy (GD-OES). The oxygen measurements suffer from atmospheric contamination signals in the first measurement seconds, which were corrected following the method described in [8]. Depth profiles of the electrically active phosphorous atomic density were determined using electrochemical capacitance-voltage profiling (ECV). It was previously observed that the poly-Si layer thickness is usually underestimated by ECV measurements, which can be attributed for with a valency correction [9]. For c-Si material a typical value of 3.77 is used, which was adjusted in this study to a value of 1.48 so that the profile depth matches the poly-Si layer thickness determined by spectral ellipsometry.

RESULTS AND DISCUSSION

Sputter Damage Compensation

After each process step, samples were taken and characterized in terms of iV_{oc}, as summarized in Fig. 1. One sample with an as-grown interfacial oxide acts as reference with iV_{oc} = 621 mV.

The a-Si sputter deposition reduces iV_{oc} by 10 mV. This behaviour is interpreted as a result of the sputter damage to the interface between the interfacial oxide and the c-Si substrate by plasma irradiation and particle bombardment.

The following high temperature anneal to partially crystallize the a-Si layer further decreases iV_{oc} to values below 600 mV. It was previously reported that, in addition to the partial crystallization of the a-Si during the high temperature anneal, local breakups of the interfacial oxide form pinholes [10]. Since the pure thermal treatment of the intrinsic sputtered a-Si layer does not provide any dopants, these pinholes might form local intrinsic poly-Si/c-Si interfaces, which could be an explanation for the loss in passivation.

The thermal treatment in N_2 atmosphere did not compensate the loss in passivation quality from the sputter damage. On the contrary, the $POCl_3$ diffused samples show higher iV_{oc} values compared to the initial passivation of the as-grown interfacial oxide reference of up to 677 mV, which can be explained by a field effect passivation.

These values can be increased by hydrogenation of the samples to passivate defects at the interface to the c-Si substrate [11]. Indeed, after deposition of a hydrogen-rich SiN_x on top of the doped poly-Si layer and a subsequent firing step, iV_{oc} is increased up to an average value of 715 mV (see Table 1). For these samples it was also possible to determine saturation current densities down to J_0 = 9 fA/cm^2, which is in the range of typical values for poly-Si/SiO_x passivating contacts [1] and might be further reduced by a process optimization focussed on J_0 rather than on sputter damage reduction.

Likewise, hydrogenation of the intrinsic samples increases iV_{oc} from below 600 mV after the thermal treatment to values, which are comparable to or higher than the ones of the as-grown interfacial oxide reference. This means

that the presence of hydrogen during the firing step is able to compensate the loss in passivation quality from the sputter damage by passivation of defects at the interface to the c-Si substrate.

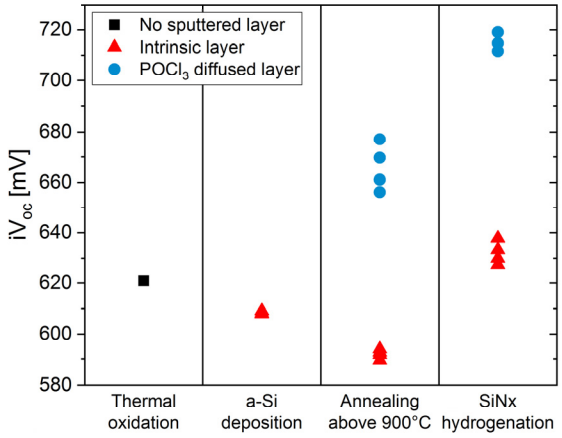

FIGURE 1. iV_{oc} after each process step. The square corresponds to the reference sample with the as-grown interfacial oxide, triangles to intrinsic layers and circles to doped layers.

TABLE 1. Summary of the average and best values of the $POCl_3$-diffused samples after SiN_x hydrogenation.

	iV_{oc} [mV]	J_0 [fA/cm²]	R_s [Ω/□]
Average	715	9.3	257
Best value	719	8.7	243

Dopant Depth Profiles

All $POCl_3$ diffused poly-Si layers show similar elemental depth profiles independent whether hydrogenated or not. Figure 2 shows these profiles for one sample exemplarily.

The most obvious observation is the difference between total (~$3\cdot10^{21}$ cm^{-3}, measured by GD-OES) and electrically active (~$5\cdot10^{20}$ cm^{-3}, measured by ECV) atomic density of phosphorous in the poly-Si layer. The ECV measured atomic density is higher than the solubility limit of electrically active phosphorous in silicon equilibrated at 900°C of roughly $3.35\cdot10^{20}$ cm^{-3} (see grey dashed horizontal line in Fig. 2) according to [12]. The determination of the temperature dependent solubility limit in [12] does include poly-Si layers from a different publication from the same authors, in which they claim that the solubility limit for single crystal silicon also holds for poly-Si [13]. From this the assumption is raised that the ECV measured atomic density has to be adjusted to lower values below the solubility limit. However, similar values above the limit were reported before without directly addressing this issue [14]. One explanation for the too high atomic density might be that the ECV etch process etches faster at grain boundaries and consequently the effectively etched area is increased. A correction for this larger etched area would lower the measured atomic densities. Due to lack of clear evidence, in this study such a correction was not applied.

The hypothesis that the ECV measured atomic density has to be adjusted in height is supported by cross-checking the electrically active atomic density of phosphorous starting from the PCD measured average sheet resistance of R_s=257 Ω/□ (see Table 1) under the assumption of a constant atomic density throughout the whole layer via the following equation:

$$n_P = (R_s \cdot \mu_e \cdot d \cdot e_0)^{-1} \quad (1)$$

With μ_e=11.4 cm^2/As the electron mobility from Hall effect measurements, d=67 nm the layer thickness and e_0 the elementary charge, the atomic density is determined to n_P=$3.18\cdot10^{20}$ cm^{-3}, which is closely below the limiting value from [12].

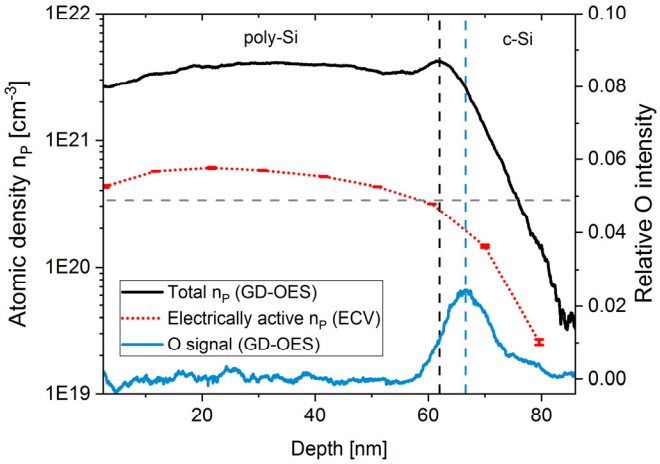

FIGURE 2. Depth profiles of a $POCl_3$-diffused sample after SiN_x hydrogenation. Total phosphorous atomic density (solid black line) and uncalibrated oxygen content (solid light blue line) measured by GD-OES. Vertical lines are the positions of the respective peak maxima. The peak in the oxygen signal represents the position of the interfacial oxide between the poly-Si layer (left) and the c-Si substrate (right). Depth profile of electrically active phosphorous atomic density measured by ECV (red error bars, dotted line as guide for the eye). The grey dashed horizontal line is the solubility limit of electrically active phosphorous atomic density in silicon equilibrated at 900°C according to [12].

The total atomic density measured by GD-OES is also higher than the solubility limit of total phosphorous atomic density in silicon of roughly $5.34 \cdot 10^{20}$ cm^{-3} according to [12]. Similarly high values were also reported before from secondary ion mass spectroscopy [15] and from secondary neutral mass spectroscopy [12]. The authors in [12] used ion implantation reaching total atomic densities of up to 10^{22} cm^{-3} and explained these high values with mobile inactive phosphorous and the formation of monoclinic SiP precipitates. Even if in the present study no ion implantation was used, the hypothesis of such additional phosphorous bonding structures could explain the high total atomic density in the GD-OES profile presented in Fig. 2.

In the oxygen signal a clear peak was measured, which originates from the interfacial oxide. The width of the peak appears with ~10 nm larger than the oxide thickness due to a loss in depth resolution with increasing measurement depth. Likewise, a pile-up of phosphorous in the GD-OES profile is observed. From the vertical lines in Fig. 2 it is evident that the phosphorous peak appears shortly before the oxygen peak, meaning that the pile-up is close to, but a few nanometers off the interfacial oxide. A similar pile-up is not observable in the depth profile of the electrically active phosphorous within the resolution of the ECV, leading to the assumption that the pile-up consists of electrically inactive phosphorous only. Such a pile-up of electrically inactive phosphorous at a Si/SiO_2 interface was reported before [16].

CONCLUSION

The a-Si deposition from rf magnetron sputtering caused a sputter damage to the interface of the poly-Si/SiO_x passivating contact. This damage was compensated by a field effect passivation after doping the a-Si layer during partial crystallization in a $POCl_3$-diffusion. For the intrinsic layers a compensation was only possible with a hydrogenation in which hydrogen is introduced to the poly-Si/SiO_x interface.

Depth profiles of the doped poly-Si layers reveal a significant difference between total and electrically active phosphorous atomic density depth profiles.. Additionally, a pile-up of electrically inactive phosphorous was observed close to, but a few nanometers off the interfacial oxide.

ACKNOWLEDGMENTS

The authors like to thank Frank Huster for helpful discussion input, Daniel Skorka for technical assistance during sputter process optimization and Lisa Mahlstaedt for wet chemical processing support. Part of this work was financially supported by the German Federal Ministry of economic affairs and energy (FKZ 0324001).

REFERENCES

1. S.W. Glunz and F. Feldmann, Sol. Energy Mat. Sol. Cells **185**, 260-269 (2018).
2. F. Haase, C. Hollemann, S. Schäfer, A. Merkle, M. Rienäcker, J. Krügener, R. Brendel and R. Peibst, Sol. Energy Mat. Sol. Cells **186**, 184-193 (2018).
3. J. Lossen, J. Hoß, S. Eisert, D. Amkreutz, M. Muske, J. Plentz and G. Andrä, in *Proc. 35rd EUPVSEC* (2018), pp. 418-421.
4. D. Yan, A. Cuevas, S. P. Phang, Y. Wan, D. Macdonald, Appl. Phys. Lett. **113** (2018).
5. G. Bräuer, B. Szyszka, M. Vergöhl and R. Bandorf, Vacuum **84**, 1354-1359 (2010).
6. L. Tutsch, M. Bivour, W. Wolke, M. Hermle and J. Rentsch, in *Proc. 33rd EUPVSEC* (2017), pp. 720-724.
7. B.-M. Meiners, D. Borchert, S. Hohage, S. Holinksi and P. Schäfer, Phys. Status Solidi A **212**, 1817-1822 (2015).
8. J. Steffens, G. Hahn and B. Terheiden, AIP Conf. Proc. **1999**, 020021-1-020021-5 (2018).
9. F. Feldmann, M. Nicolai, R. Müller, C. Reichel and M. Hermle, Energy Procedia **124**, 31-37 (2017).
10. G. R. Wolstenholme, N. Jorgensen, P. Ashburn and G. R. Booker, J. Appl. Phys. **61** (1), 225-233 (1987).
11. S. Mack, J. Schube, T. Fellmeth, F. Feldmann, M. Lenes and J.-M. Luchies, Phys. Status Solidi RRL **11**, 1700334 1-4 (2017).
12. S. Solmi, A. Parisini, R. Angelucci and A. Amigliato, Phys. Rev. B **53** (12), 7836-7841 (1996).
13. A. Carabelas, D. Nobili and S. Solmi, J. Phys. Colloques **43** (C1), 187-192 (1982).
14. M. K. Stodolny, J. Anker, B. L. J. Geerligs, G. J. M. Janssen, B. W. H. van de Loo, J. Melskens, R. Santbergen, O. Isabella, J. Schmitz, M. Lenes, J.-M. Luchies, W. M. M. Kessels and I. Romijn, Energy Procedia **124**, 635-642 (2017).
15. A. Liu, D. Yan, J. Wong-Leung, L. Li, S. P. Phang, A. Cuevas and D. Macdonald, ACS Appl. Energy Mater. **1**, 2275-2282 (2018).
16. F. Lau, L. Mader, C. Mazure, Ch. Werner and M. Orlowski, Appl. Phys. A **49**, 671-675 (1989).